



**HAL**  
open science

## Antisolvent crystallization of a cardiotoxic drug in ionic liquids: Effect of mixing on the crystal properties

Jacqueline Resende de Azevedo, Fabienne Espitalier, Jean-jacques Letourneau, Maria-Inês Ré

### ► To cite this version:

Jacqueline Resende de Azevedo, Fabienne Espitalier, Jean-jacques Letourneau, Maria-Inês Ré. Antisolvent crystallization of a cardiotoxic drug in ionic liquids: Effect of mixing on the crystal properties. *Journal of Crystal Growth*, 2017, Industrial Crystallization and Precipitation in France (CRISTAL-8), May 2016, Rouen (France), 472 (SI), pp.29-34. 10.1016/j.jcrysgr.2016.12.057 . hal-01619261

**HAL Id: hal-01619261**

**<https://hal.science/hal-01619261>**

Submitted on 5 Sep 2018

**HAL** is a multi-disciplinary open access archive for the deposit and dissemination of scientific research documents, whether they are published or not. The documents may come from teaching and research institutions in France or abroad, or from public or private research centers.

L'archive ouverte pluridisciplinaire **HAL**, est destinée au dépôt et à la diffusion de documents scientifiques de niveau recherche, publiés ou non, émanant des établissements d'enseignement et de recherche français ou étrangers, des laboratoires publics ou privés.

# Antisolvent crystallization of a cardiotoxic drug in ionic liquids: Effect of mixing on the crystal properties

Resende de Azevedo Jacqueline, Espitalier Fabienne\*, Letourneau Jean-Jacques, Ré Maria Inês

Université de Toulouse, Mines Albi, CNRS, Centre RAPSODEE, Campus Jarlard, F-81013 Albi CT cedex 09, France

## ABSTRACT

LASSBio-294 (3,4-methylenedioxybenzoyl-2-thienylhydrazon) is a poorly soluble drug which has been proposed to have major advantages over other cardiotoxic drugs. Poorly water soluble drugs present limited bioavailability due to their low solubility and dissolution rate. An antisolvent crystallization processing can improve the dissolution rate by decreasing the crystals particle size. However, LASSBio-294 is also poorly soluble in organic solvents and this operation is limited. In order to open new perspectives to improve dissolution rate, this work has investigated LASSBio-294 in terms of its antisolvent crystallization in 1-ethyl-3-methylimidazolium methyl phosphonate [emim][CH<sub>3</sub>O(H)PO<sub>2</sub>] as solvent and water as antisolvent. Two modes of mixing are tested in stirred vessel with different pre-mixers (Roughton or T-mixers) in order to investigate the mixing effect on the crystal properties (crystalline structure, particle size distribution, residual solvent and in vitro dissolution rate). Smaller drug particles with unchanged crystalline structure were obtained. Despite the decrease of the elementary particles size, the recrystallized particles did not achieve a better dissolution profile. However, this study was able to highlight a certain number of findings such as the impact of the hydrodynamic conditions on the crystals formation and the presence of a gel phase limiting the dissolution rate.

### Keywords:

Poorly water-soluble drug  
Ionic liquids  
Antisolvent crystallization  
Dissolution enhancement

## 1. Introduction

Poorly soluble drugs present limited bioavailability due to their low solubility and dissolution rate, and several strategies have been developed in order to find ways to improve them. Crystallization techniques are widely used in the pharmaceutical industry and antisolvent crystallization has been used to reduce the particle size in order to increase drug dissolution rate [1–3]. In this method, the drug is dissolved in the solvent and the formed solution is poured to the antisolvent. This mixing generates high supersaturation that subsequently induces nucleation, simultaneous growth, and possibly agglomeration of crystals. The properties of the final crystalline product such as size, morphology and purity are significantly dependent on the rate, magnitude and uniformity of supersaturation generated during crystallization. Fig. 1 summarizes the main operating parameters and phenomena (nucleation, growth and agglomeration) influencing the crystals properties.

Pharmaceutical drugs are generally crystallized from organic solutions using an antisolvent crystallization technique. However, there is a general consensus in limiting the use of organic solvents because of their negative environmental and health impact. The introduction of alternative solvents such as supercritical fluids [4] and ionic liquids [5–10] opens new opportunities for the pharmaceutical industry, and also

reduces the disadvantages of traditional volatile organic compounds.

Ionic liquids (ILs) are solvents that consist entirely of ions, differently from molecular solvents consisting of only neutral molecules and salt solutions consisting of ions and molecules. ILs are composed of a relatively large asymmetric organic cation and an inorganic or organic anion. The asymmetry of the cation is responsible for low lattice energies of ILs and their liquid state at ambient conditions. In general, they are thermally stable, nonflammable and exhibit very low vapor pressure. The application of ionic liquids as solvents in the crystallization processing of pharmaceutical drugs is still relatively unexplored, which results in a low number of studies in the literature. To the best of our knowledge, the drugs concerned by these studies are methyl-(Z)- $\alpha$ -acetamidocinnamate [4], paracetamol [11–13], ibuprofen and flufenamic acid [12], adefovir dipivoxil [14,15], rifampicin [9] and vancomycin [16]. Among them, the antisolvent crystallization of rifampicin using 1-ethyl-3-methylimidazolium methyl phosphonate [emim][CH<sub>3</sub>O(H)PO<sub>2</sub>] resulted in ultrafine amorphous particles with faster dissolution rate.

LASSBio-294 (3,4-methylenedioxybenzoyl-2-thienylhydrazon) is a new bioactive molecule which has been proposed in an attempt to develop new therapies to simplify the treatment of cardiovascular diseases [17,18]. However, as a hydrophobic drug, it exhibits a low solubility and dissolution rate in the gastro-intestinal tract, which

\* Corresponding author.

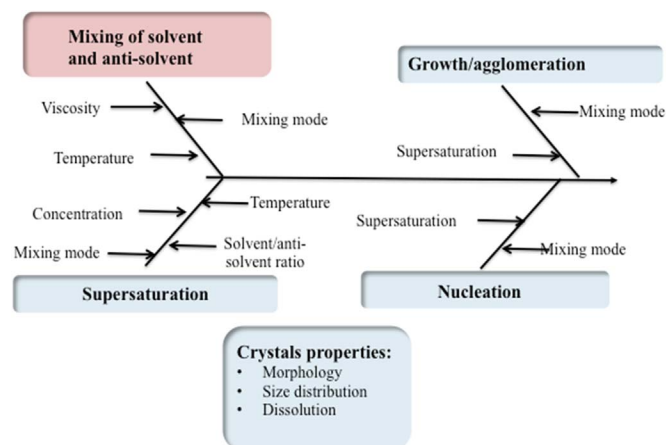


**Fig. 1.** Main operating parameters (mixing and supersaturation) and phenomena (nucleation, growth and agglomeration) having an impact on crystals properties.

limits its effective absorption and bioavailability after oral administration. An improvement of the bioavailability should reduce considerably the dose of the drug to be administered.

Antisolvent crystallization has been used to improve dissolution rate by decreasing the drug crystals particle size. For pharmaceutical drugs poorly soluble also in organic solvents such as LASSBio-294 this operation is limited. However, our group has determined the solubility of LASSBio-294 in seven different imidazolium based ionic liquids and in binary mixtures of water/ILs and this compound showed sufficient solubility in five of the tested ILs, 1-ethyl-3-methylimidazolium methyl phosphonate [emim][CH<sub>3</sub>O(H)PO<sub>2</sub>] among them [19]. Based on these results, the objective of the present study was to investigate LASSBio-294 in terms of its antisolvent crystallization in 1-ethyl-3-methylimidazolium methyl phosphonate [emim][CH<sub>3</sub>O(H)PO<sub>2</sub>] as solvent and water as antisolvent and under various preparation conditions. The influence of the mixing mode of the drug solution (ionic liquid-drug) and the antisolvent (water) and the solute concentration in the solvent have been studied. In order to get a fast and homogeneous mixing to obtain uniform distribution of concentration and so small crystals, two pre-mixers (Roughton and T-mixer) were used. A reference experiment without pre-mixer was conducted for comparison. The end crystals properties are particle size distributions, crystalline structure, residual solvent in crystals and in vitro dissolution.

## 2. Materials and methods

### 2.1. Materials

The LASSBio-294 was obtained from Cristália Ltda (Itapira, SP, Brazil) and used without further purification. It is in the form of a yellowish solid with a molecular weight of 274.3 g/mol and 99.96% purity. The ionic liquid, 1-ethyl-3-methylimidazolium methyl phosphonate ([emim][CH<sub>3</sub>O(H)PO<sub>2</sub>]), was obtained from Solvionic (Toulouse, France) and it was used as received (>98% pure). Sodium dodecyl sulfate (SDS) was supplied by VWR International

(Leuven, Belgium). HPLC grade acetonitrile (Scharlau SL, Spain), methanesulfonic acid (MSA) (Fluka, Buchs, Switzerland) for ion chromatography were used to prepare the mobile phases. Sodium dihydrogen phosphate (NaH<sub>2</sub>PO<sub>4</sub>) (Sigma-Aldrich, Gillingham-Dorset, England) and sodium hydrogen phosphate (Na<sub>2</sub>HPO<sub>4</sub>) (Alfa Aesar, Karlsruhe, Germany) of analytical grade were used to prepare the buffers and mobile phases. Water was distilled and purified using Milli-Q Water Purification System (Purelab Classic DI MK2, Elga, UK).

### 2.2. Methods

#### 2.2.1. Crystallization method

First, a LASSBio-294 solution with defined concentration (57, 91 or 159 ± 1 mg LASSBio-294/g solution) was prepared in [emim][CH<sub>3</sub>O(H)PO<sub>2</sub>] as solvent at 30 ± 0.5 °C. The anti-solvent crystallization was conducted in a stirred vessel. The stirred vessel has a volume of 200 mL (diameter 6.3 cm), with double jacket equipped with a mechanical turbine stirrer with 8 blades mounted on flat disc throughout the operation. The temperature at 25 ± 0.5 °C was controlled by a water bath (Julabo VC F30). Agitation at 800 rpm was powered using a mechanical stirrer (Eurostar IKA laborotechnick 2000 motor). Based on preliminary tests and solid-liquid equilibrium of our ternary system, mass ratios water/[emim][CH<sub>3</sub>O(H)PO<sub>2</sub>] between 12.5 and 13.9 were used (Azevedo, 2014). After 30 min, the particle size distributions were determined. The suspension resulted was filtered (pore size 0.2 µm, polypropylene, Milipore, Bedford, MA, UK). The filter cake was washed with water (500g) to remove the residual solvent. The crystals were dried in vacuum oven (Heraeus Vacutherm-VT-6025) at 50 °C for 3–5 days and then further characterized in terms of crystal structure, morphology, residual solvent and in vitro dissolution. Operating conditions are given in Table 1.

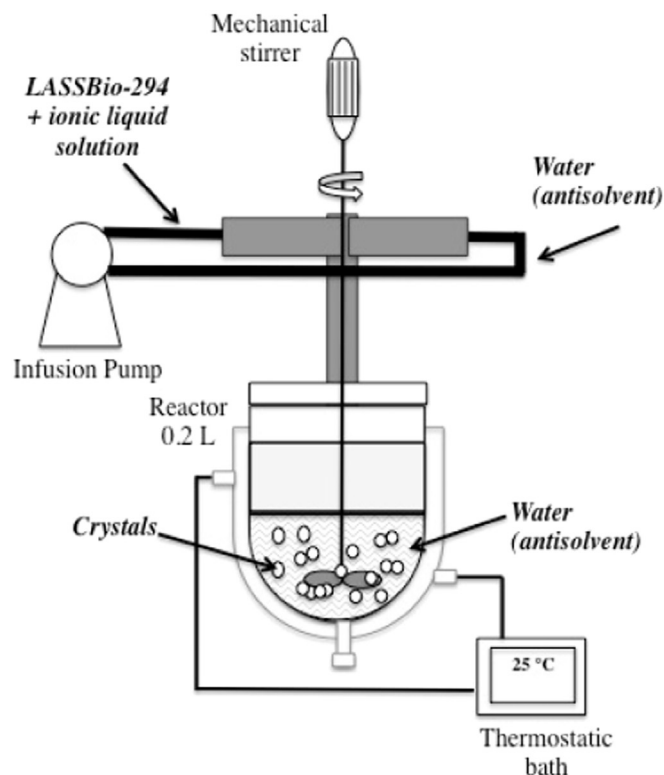
Two mixing mode of solution and antisolvent were tested:

- Indirect addition: the simultaneous addition of the LASSBio-294-[emim][CH<sub>3</sub>O(H)PO<sub>2</sub>] solution and water in stirred vessel is carried with a pre-mixer (Fig. 2(a)). Initially, water is present in the stirred vessel in order to allow agitation of the suspension leaving the pre-mixer. Note that it induces the creation of a new supersaturation. Two types of pre-mixers, Roughton and T-mixer, were manufactured on the basis of the work of Lindenberg et al. [20]. The Roughton mixer has an inlet tube of 1 mm diameter, a mixing chamber diameter of 3 mm and its outlet tube a diameter of 1.75 mm and a length of 15 mm (Fig. 2(b)). The T-mixer has two radial entries with a diameter of 1 mm and its outlet tube has a diameter of 2 mm with a length of 17.5 mm (Fig. 2(c)). Organic and aqueous phases were introduced into the pre-mixer with an infusion pump (Harvard PHD 2000 Infusion, USA) at 40 mL/min. The maximum supersaturation ratio into pre-mixer is noted S<sub>pre-mixer</sub> (Table 2).
- Direct addition: the organic solution is introduced rapidly into a stirred vessel containing water. The maximum supersaturation ratio into stirred vessel is noted S<sub>stirred vessel</sub> (Table 2).

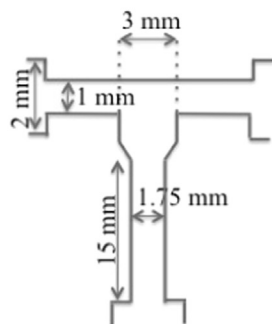
**Table 1**

Process conditions and products characteristics.

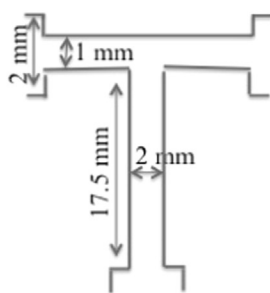
Experiment number	Raw drug	1	2	3	4	5
Concentration (mg/g solution)		159	159	159	91	57
Water/IL ratio		13.7	13.7	13.9	13.0	12.5
Mixing mode		Roughton	T-mixer	Without mixer	Roughton	Roughton
Residual solvent (ppm)	0	23644	19470	6920	4271	2708
D <sub>4,3</sub> (± 1) (µm)	57.9	9.0	8.0	14.0	9.0	6.0
D <sub>3,2</sub> (± 1) (µm)	29.5	2.0	2.0	3.0	2.0	1.5
Crystallization yield (%)		93.0	88.0	91.1	95.3	85.1



(a)



(b)



(c)

**Fig. 2.** Scheme of the experimental process to prepare LASSBio-294 particles with pre-mixer (a) and illustrations of the Roughout (b) and (c) T pre-mixers.

## 2.2.2. Characterization of products

**2.2.2.1. Particle size analysis.** Mean particle size and particle size distribution were determined by laser diffraction using a Mastersizer 3000 (Malvern Instruments, UK). At the end of synthesis (30 min), a few drops of suspension were added directly into the tank of the laser diffractometry containing water until the laser obscuration level was in the desired range (5–15%). A refractive index of 1.520 was used for the particles (by default use) and 1.33 for the continuous phase (water). The samples circulated in the measuring cell using the instrument's internal stirring system (2200 rpm) and with the help of an ultrasonic probe. Results were expressed as volume percentage (%) according to the particle size diameter ( $\mu\text{m}$ ). The mean surface diameter,  $D_{3,2}$ , and mean volume diameter,  $D_{4,3}$ , calculations were done by using the Malvern 3000 software version 3.20 supplied by the manufacturer (Malvern Instruments Ltd).

**2.2.2.2. Scanning electron microscopy (SEM).** The morphology of

**Table 2**

$t_{\text{ind}}$  and  $t_{\text{mix}}$  values into the pre-mixer and the stirred vessel.

Experiments number	Pre-mixer			Stirred vessel			
	$S_{\text{pre-mixer}}$	$t_{\text{ind}} \cdot 10^4$ (ms)	$t_{\text{mix}}$ (ms)	$S_{\text{stirred vessel}}$	$t_{\text{ind}} \cdot 10^4$ (ms)	$Re_A$	$t_{\text{mix}}$ (s)
1	8126	1.27	0.292 <sup>***</sup>				
2	8443	1.26	>				
3	–	–	0.292 <sup>**</sup>	14918	0.62	1801	1.21 <sup>****</sup>
4	4256	1.38	0.294 <sup>***</sup>				
5	2451	1.48	0.299 <sup>***</sup>				

Properties used:

\* Diffusion coefficient of the LASSBio =  $9.6 \times 10^{-11} \text{ m}^2/\text{s}$  into stirred vessel and  $4.9 \times 10^{-11} \text{ m}^2/\text{s}$  into the pre-mixer, diameter molecular of the solute =  $8.4 \times 10^{-10} \text{ m}$ .

\*\* Not calculated.

\*\*\* Kinematic viscosity after complete mixing:  $10^{-5} \text{ m}^2/\text{s}$  and average speed: 0.52 m/s.

\*\*\*\* Diameter of the stirred vessel: 0.063 m, Diameter of the agitator: 0.027 m, Liquid height: 0.05 m, Agitation rate: 800 rpm, Dynamic viscosity:  $5 \cdot 10^{-3} \text{ Pa}\cdot\text{s}$ , Volume of the solution: 0.146 L, Power number of the agitator (function of the Reynolds number of the agitator  $Re_A$ ): 4. Despite an intermediate hydrodynamic regime ( $10 < Re_A < 10^4$ ), a constant power number and equal to 4 was chosen. Indeed, in the Reynolds number range of our agitator, this number varies little with power [21].

powder samples was visualized using an Environmental Scanning Electron Microscope-Field Emission Gun microscope (Philips XL30 FEG, ESEM-FEG, FEI Company). The samples were fixed on an SEM stub using double-sided adhesive tape and coated with platinum using a Polaron SC7640 high resolution SEM sputter coater (Quorum Technologies, England). Images were taken with an accelerating voltage of 20 kV.

**2.2.2.3. X-ray diffractometry (XRD).** The samples were carried out using XRD diffractometry (Philips X'Pert diffractometer, PanAnalytical, USA). The measurements were performed using  $\text{CuK}\alpha$  radiation at a scanning rate of  $0.018^\circ/\text{min}$  from  $8$  to  $40^\circ$ , applying 45 kV and 40 mA. The diffraction patterns were collected in an angular range ( $2\theta$ ) of  $10$ – $35^\circ$ .

**2.2.2.4. Residual solvent.** A Dionex model ICS-3000 ion chromatograph was applied for determining residual solvent in the crystal by the quantification of cation-IL. This system consists of an autosampler, a degasser, pumps and conductometric detector. A Dionex suppressor LERS 500 (4 mm) for chemical suppression was installed between the conductometric detector and the Dionex IonPac CS17 analytical column (250 mm x 4 mm). A Dionex IonPac CG17 (50 mm x 4 mm) guard column was also installed. The samples were eluted by isocratic elution with acetonitrile-MSA 20 mM mixtures (20:80 (w/w)) at a flow rate of 1.0 mL/min. An injection volume of 25  $\mu\text{L}$  was used. All chromatographic analyses were carried at  $35 \pm 0.5^\circ\text{C}$ . Cation-IL concentration in the crystals was determined from solutions prepared with 100% acetonitrile. The concentrations were calculated with linear regression equation (Peak area ( $\mu\text{S}/\text{min}$ ) =  $0.0165 C (\mu\text{g}/\text{g solution}) - 0.0495$ ,  $R^2 = 0.9954$ ) obtained with the linear ranges of calibration curve between peak area and the concentration (0.6–144  $\mu\text{g}/\text{g solution}$ ).

**2.2.2.5. Dissolution.** Dissolution studies were performed assuring sink-conditions (maximal concentration lower than the third of the equilibrium concentration) according to the paddle method (USP) using an Erweka DT60 dissolution apparatus (Erweka, Germany). The stirring speed used was 50 rpm, and the temperature was maintained at  $37 \pm 0.5^\circ\text{C}$  ( $n=3$ ). The dissolution medium (900g) was phosphate buffer pH 7.4 containing SDS 0.5%. This phosphate buffer consisted of

a mixture 1.2% sodium dihydrogen phosphate ( $\text{NaH}_2\text{PO}_4$ ) and 8.8% sodium hydrogen phosphate ( $\text{Na}_2\text{HPO}_4$ ). An accurately weighed quantity of each sample equivalent to 14 mg of LASSBio-294 was used to the experiment (calculated from the LASSBio-294 solubility in SDS 0.5% pH 7.4 equals to about 0.046 mg/g solution). Samples were taken at an appropriate time interval. Samples were filtered through a 0.2  $\mu\text{m}$  filter (Acrodisc GHP, Milipore, Bedford, MA, UK) and analyzed by HPLC. The HPLC analyses were carried with a system consisted of an Agilent chromatograph (Model 1100 series) equipped with a UV-Vis detector. A reversed phase analytical Symmetry® C18 column, 100 Å, 5  $\mu\text{m}$  (4.6 mm x 250 mm, WAT054275, Waters) was maintained at room temperature and equilibrated with the analytical mobile phase before injection. The mobile phase consisted of a mixture of 20% acetonitrile and 80% phosphate buffer (0.02 mol  $\text{NaH}_2\text{PO}_4/\text{L}$  with phosphoric acid 1%, pH of 4.5). The flow rate was 1.0  $\text{cm}^3/\text{min}$ , the elution was monitored at 318 nm, and the injection volume was 0.02  $\text{cm}^3$ . The concentrations were calculated with linear regression equation (Peak area (mAU) = 61.971 C ( $\mu\text{g}/\text{g}$  solution) - 15.129,  $R^2=0.9990$ ) obtained with the linear ranges of calibration curve (0.6–81  $\mu\text{g}/\text{g}$  solution). The percentage of the dissolved drug was calculated with the ratio between LASSBio-294 dissolved mass for a given time and LASSBio-294 initial mass.

### 3. Results and discussion

The experiments were designed to determine, at the end of synthesis, the influence of the mixing mode and the initial solute (drug) concentration on the following properties of the dry solid: particle size distribution, morphology and residual solvent. The experimental yields are higher than 85% but less than the theoretical yield of 99% (Table 1). The theoretical yield is calculated from a mass balance assuming that, in the end of the operation and at the experiment temperature, the solution is saturated. The difference between theoretical and experimental yields is partly caused by the solid's waste into the stirred vessel. X-ray powder diffractograms (Fig. 3) showed that the synthesized LASSBio-294 is crystalline like the raw drug, even if changes in peak relative intensities could be observed in  $2\theta$  range 24–27° [22].

#### 3.1. Influence of the mixing mode

The influence of the mixing mode is observed with experiments 1, 2 and 3 (Table 1). The mean sizes of the dry solid ( $D_{4,3}$  and  $D_{3,2}$ ) are smaller than the initial solid ( $D_{4,3}=57.9 \mu\text{m}$  and  $D_{3,2}=29.5 \mu\text{m}$ ). The mean volume size ( $D_{4,3}$ ) obtained without pre-mixer is higher than those obtained with pre-mixer, but the amount of residual solvent is lower (6920 ppm against amounts higher than 19470 ppm). The mean surface size ( $D_{3,2}$ ) is unchanged. Particle size distributions and

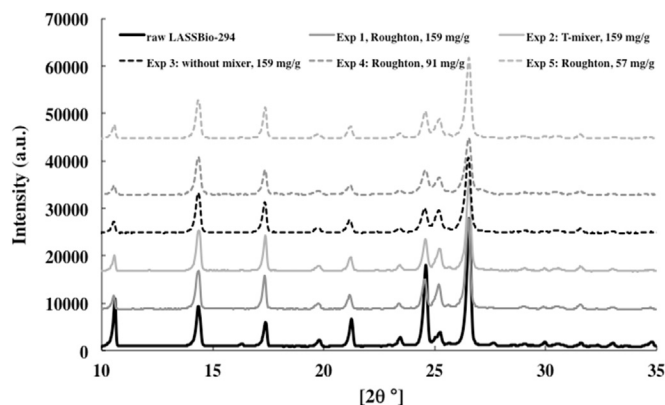


Fig. 3. X-ray powder diffractograms of raw LASSBio-294 and recrystallized samples.

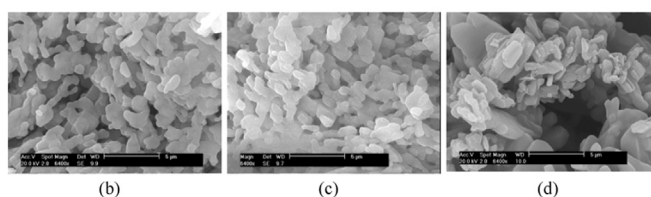
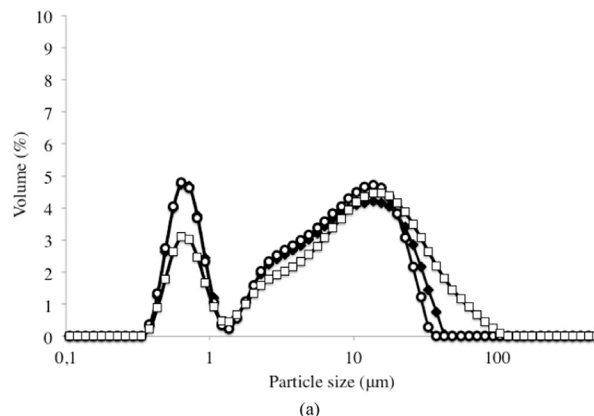


Fig. 4. Particles size distribution and SEM images for recrystallized LASSBio-294: Influence of the mixing mode. Roughton mixer, experiment 1 (a) filled diamond and (b) with 23 644 ppm at residual solvent; T-mixer, experiment 2 (a) empty circle and (c) with 19 470 ppm at residual solvent; Without pre-mixer, experiment 3 (a) empty square and (d) with 6920 ppm at residual solvent.

morphologies of the crystals after 30 min of the synthesis are shown in Fig. 4. They present a first peak of less than 1  $\mu\text{m}$  and a second one between 12 and 100  $\mu\text{m}$  corresponding to at least two populations (Fig. 4(a)). Observing the SEM images, the first peak could be attributed to the elementary particles and the second one to the agglomerates. The first peak seems to have always the same width, only its intensity varies: it is identical when using a pre-mixer and less intense when working with a direct addition. SEM images also show that the crystal habit appears to be related to some residual solvent content (Fig. 4(b), (c), (d)): Higher the residual solvent, less defined the edges of the crystals. Therefore, the crystals have a waxy appearance, as already observed in the case of rifampicin [9].

#### 3.2. Influence of the initial drug concentration with pre-mixer

The study of the drug concentration in solution was performed with the Roughton mixer (experiments 1, 4 and 5, Table 1). The mean sizes ( $D_{4,3}$  and  $D_{3,2}$ ) are identical for two different conditions (91 and 159 mg LASSBio-294/g solution) and slightly lower for the third condition (57 mg LASSBio-294/g solution). The bimodal particle size distributions are shown in Fig. 5. The intensity of the first peak decreases by increasing the initial concentration; in contrast, the second peak remains unchanged regardless the concentration (Fig. 5(a)). Increase of the first peak intensity comes primarily from the supersaturation increase, which induces an increase of the nucleation rate when increasing the initial concentration. The  $S_{\text{pre-mixer}}$  ranges between 2400 and 8200 (Table 2). The residual solvent decreases as the initial concentration decreases. The crystal habit is always related to some residual solvent content (Fig. 5(b), (c), (d)).

#### 3.3. Mixing time and crystals formation mechanism

The mixing time,  $t_{\text{mix}}$  (s), into Roughton mixer and the macromixing time into the stirred vessel ( $t_{\text{macro, turbulent}}$ ) were estimated and compared with the induction time ( $t_{\text{ind}}$ ). The  $t_{\text{mix}}$  (s) into Roughton mixer is calculated from the equation [20]:

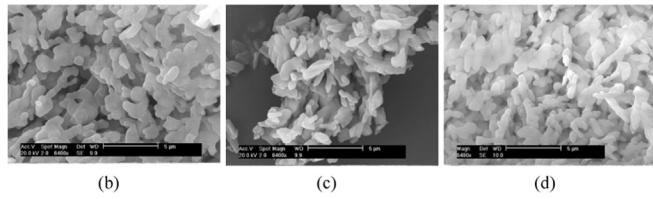
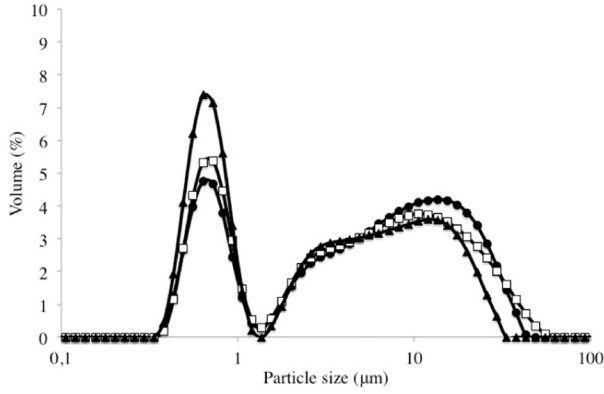


**Fig. 5.** Particles size distribution and SEM images for recrystallized LASSBio-294: influence of the initial drug concentration. 159 mg/g, experiment 1 (a) filled circle and (b) with 23 644 ppm at residual solvent; 91 mg/g, experiment 4 (a) empty square and (c) with 4 271 ppm at residual solvent; 57 mg/g, experiment 5 (a) filled triangle and (d) with 2 708 ppm at residual solvent.

$$t_{mix} = 1100 \frac{d_j^{0.5} \nu^{0.5}}{u_j^{1.5}} \quad (1)$$

where  $d_j$  is the inlet diameter in the pre-mixer (1 mm),  $\nu$  the kinematic viscosity after complete mixing and  $u_j$  the average speed. For a solvent/anti-solvent ratio different from 1,  $u_j$  is calculated assuming an equivalent kinetic energy.

For the calculation of the  $t_{macro, turbulent}$  into stirred vessel, it was assumed a complete mixing of the two solutions without considering the solid formation (% solid mass to the final time < 2). It is obtained by the following relationship [23]:

$$t_{macro, turbulent} = 7.3 \left( \frac{T^2}{\bar{\epsilon}} \right)^{1/3} \quad (2)$$

where  $\bar{\epsilon}$  is the average power (W) calculated by  $\bar{\epsilon} = \frac{4}{\pi} N_p u^3 D^2 \left( \frac{D}{T} \right)^2 \frac{D}{H}$  with  $u$  the rotation speed of the agitator ( $s^{-1}$ ),  $N_p$  the power number of the agitator,  $D$  the diameter of agitator (m),  $H$  the liquid height into the stirred vessel (m) and  $T$  the vessel diameter (m).

Macromixing time will be greater in the case of a laminar flow. The  $t_{ind}$  (s) was estimated from the molecular diameter of the solute  $d_m$  (m), the supersaturation  $S$  and the diffusion coefficient  $D_{AB}$  ( $m^2/s$ ) [23]:

$$t_{ind} = \frac{80 d_m^2}{D_{AB} \ln(S)} \quad (3)$$

In all cases, given the supersaturation values, the  $t_{ind}$  ( $10^{-4}$  ms) were very low compared with the  $t_{mix}$ . Therefore, it could be concluded that the crystal formation process is controlled by the mixing between drug solution and antisolvent.

During the solubility studies, it was found that a gel phase could be formed beyond a certain solute concentration in the ionic liquid [19]. The appearance of crystals observed on the SEM images suggests that the particles obtained are fluid aggregates frozen from a completely segregated mixture. These particles would consist of a gel phase being formed during the mixing of the two phases, however, a crystalline phase was detected by X-ray diffraction. Washing the crystals with a greater quantity of water can change crystal habit. It seems that the gel phase is present at crystals surface.

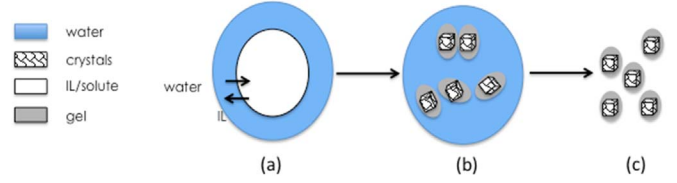


**Fig. 6.** Mechanism of formation of crystals: (a) mixing and transfer of solvent and anti-solvent, (b) formation of crystals and gel, (c) decrease of phase gel after washing.

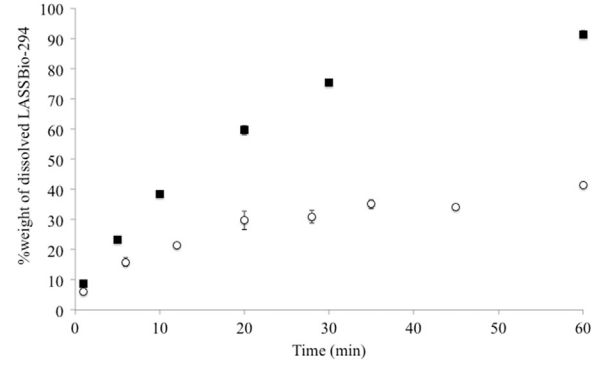


**Fig. 7.** Dissolution kinetic profiles for raw and recrystallized LASSBio-294 (testing conditions: SDS 0.5%, pH 7.4 at  $37 \pm 0.5$  °C, n=3). Filled square (raw LASSBio-294), Empty circle (recrystallized LASSBio-294, Experiment 1).

It would also seem that when the mixing is fast and the initial LASSBio-294 concentration is high, the residual solvent in the final particles is higher. From our experiments we show that, during the process, crystals and gel are formed due to the mixing of the two phases (Fig. 6). It is not possible to determine what phases are formed first. An intense mixing and high concentration of solute seems to favor the gel formation.

### 3.4. Dissolution studies

The in vitro dissolution profiles of raw and recrystallized LASSBio-294 (Experiment 1, residual solvent highest) are compared in Fig. 7. The in vitro dissolution tests were carried out in triplicate. The standard deviation calculated was reported on the figure. The recrystallized LASSBio-294 dissolved significantly slower than the raw LASSBio-294. Both profiles are statistically different for 60 min dissolution test. For example, after 30 min, 31% of the recrystallized drug and 75% of the original crystals are dissolved. The LASSBio-294 is very slightly soluble in water. Its solubility in aqueous medium with SDS 0.5% is improved by micellar solubilisation. Furthermore, the presence of the surfactant reduces the solid-liquid interfacial tension and increases the LASSBio-294 crystals wettability. These effects enhance the dissolution of the LASSBio-294 and could explain the high dissolution rate of the original crystals. Despite a lower mean size, the slower dissolution of the recrystallized drug can be explained by the gel phase presence, which probably slowed the mass transfer and therefore the aggregates dissolution.

## 4. Conclusion

In the present study we examined the antisolvent crystallization of a new hydrophobic drug using an ionic liquid as solvent. Despite obtaining a finer powder, the recrystallized drug in vitro dissolution is slower than that of the unprocessed drug crystals. This behavior could be due to a gel phase formation when the drug solution is mixed with the antisolvent. This gel phase induces the appearance of aggregates which are difficult to disperse. A rapid mixing and high initial drug concentration in the organic phase seem favors the gel phase formation and leads to the formation of synthesized particles

with a poorer dissolution.

ILs open new opportunities for the pharmaceutical industry as alternative solvents. However they introduce new difficulties into an antisolvent crystallization method related to the presence of a new gel phase (not observed in the presence of traditional volatile organic solvents) that can slower the dissolution of the recrystallized drug particles even if are smaller in size. Its formation is a limiting parameter and has to be controlled in the process. Therefore, the use of ionic liquids can open future investigations for the pharmaceutical drugs recrystallization keeping in mind the need of control of the gel phase formation. New ways along this line to limit the gel phase formation could be a direct addition of the drug solution in the antisolvent phase. This mode of addition would allow each drop of organic solution to disperse more easily into the aqueous phase before the gel phase formation. Our work in going on to check for these assumptions.

### Acknowledgment

The authors would like to thank Cristália Ltda (Itapira, São Paulo, Brazil) for providing the drug LASSBio-294 and CNPq (Brazilian National Research Council) for doctoral fellowship to ResendeAzevedo J. (Proc.200835/2010-6).

### References

- [1] H. Zhao, J.-X. Wang, Q.-A. Wang, J.-F. Chen, J. Yun, Controlled liquid antisolvent precipitation of hydrophobic pharmaceutical nanoparticles in a microchannel reactor, *Ind. Eng. Chem. Res.* 46 (2007) 8229–8235.
- [2] H.X. Zhang, J.X. Wang, Z.B. Zhang, Y. Le, Z.G. Shen, J.F. Chen, Micronization of atorvastatin calcium by antisolvent precipitation process, *Int. J. Pharm.* 374 (2009) 106–113.
- [3] Y. Dong, W.K. Ng, S. Shen, S. Kim, R.B.H. Tan, Preparation and characterization of spironolactone nanoparticles by antisolvent precipitation, *Int. J. Pharm.* 375 (2009) 84–88.
- [4] M.C. Kroon, V.A. Toussaint, A. Shariati, L.J. Florusse, J. van Spronsen, G.-J. Witkamp, C.J. Peters, Crystallization of an organic compound from an ionic liquid using carbon dioxide as anti-solvent, *Green Chem.* 10 (2008) 333–336.
- [5] H. Mizuuchi, V. Jaitely, S. Murdan, A.T. Florence, Room temperature ionic liquids and their mixtures: potential pharmaceutical solvents, *Eur. J. Pharm. Sci.* 33 (2008) 326–331.
- [6] K.B. Smith, R.H. Bridson, G.A. Leeke, Solubilities of pharmaceutical compounds in ionic liquids, *J. Chem. Eng. Data* 56 (2011) 2039–2043.
- [7] C. Lourenço, C.I. Melo, R. Bogel-Lukasik, E. Bogel-Lukasik, Solubility advantage of Pyrazine- 2-carboxamide: application of alternative solvents on the way to the future pharmaceutical development, *J. Chem. Eng. Data* 57 (2012) 1525–1533.
- [8] A. Forte, C.I. Melo, R. Bogel-Lukasik, E. Bogel-Lukasik, A favourable solubility of isoniazid, an antitubercular antibiotic drug, in alternative solvents, *Fluid Phase Equilib.* 318 (2012) 89–95.
- [9] A. Viçosa, J.-J. Letourneau, F. Espitalier, M.I. Ré, An innovative antisolvent precipitation process as a promising technique to prepare ultrafine rifampicine particles, *J. Cryst. Growth* 342 (2012) 80–87.
- [10] C.I. Melo, R. Bogel-Lukasik, M. Nunes daPonte, E. Bogel-Lukasik, Ammonium ionic liquids as green solvents for drugs, *Fluid Phase Equilib.* 338 (2013) 209–216.
- [11] K.B. Smith, R.H. Bridson, G.A. Leeke, Crystallisation control of paracetamol from ionic liquids, *Cryst. Eng. Comm.* 16 (2014) 10797–10803.
- [12] K.B. Smith, Crystallisation of active pharmaceutical ingredients using ionic liquids, Thesis, School of Chemical Engineering, Faculty of Engineering, University of Birmingham, Royaume-Uni, 2015.
- [13] C.C. Weber, S.A. Kulkarni, A.J. Kunov-Kruse, R.D. Rogers, A.S. Myerson, The use of cooling crystallization in an ionic liquid system for the purification of pharmaceuticals, *Cryst. Growth Des.* 15 (2015) 4946–4951.
- [14] J.H. An, J.M. Kim, S.M. Chang, W.S. Kim, Application of ionic liquid to polymorphic design of pharmaceutical ingredients, *Cryst. Growth Des.* 10 (2010) 3044–3050.
- [15] J.-H. An, W.-S. Kim, Antisolvent crystallization using ionic liquids as solvent and antisolvent for polymorphic design of active pharmaceutical ingredient, *Cryst. Growth Des.* 13 (2013) 31–39.
- [16] G.S. Ha, J.-H. Kim, Effect of an ionic liquid on vancomycin crystallization, *Korean J. Chem. Eng.* 32 (2015) 576–582.
- [17] P.C. Lima, L.M. Lima, K.C.M. da Silva, P.H.O. Léda, A.L.P. de Miranda, C.A.M. Fraga, et al., Synthesis and analgesic activity of novel N-acylarylhydrazones and isosters, derived from natural safrole, *Eur. J. Med. Chem.* 35 (2000) 187–203.
- [18] E.J. Barreiro, Estratégia de simplificação molecular no planejamento racional de fármacos: a descoberta de novo agente cardioprotetor, *Quim. Nova.* 25 (2002) 1172–1180.
- [19] J.R. Azevedo, J.-J. Letourneau, F. Espitalier, M.I. Ré, Solubility of a new cardioactive prototype drug in ionic liquids, *J. Chem. Eng. Data* 59 (2014) 1766–1773.
- [20] C. Lindenberg, J. Schöll, L. Vicum, M. Mazzotti, J. Brozio, Experimental characterization and multi-scale modeling of mixing in static mixers, *Chem. Eng. Sci.* 63 (2008) 4135–4149.
- [21] P. Trambouze, J.-P. Euzen, Les récepteurs chimiques: de la conception à la mise en oeuvre, Technip, Paris, 2002.
- [22] J.R. Azevedo, Etude de la cristallisation d'une nouvelle molécule à efficacité cardiotonique dans un mélange liquide ionique – eau, Thèse, Génie des procédés et de l'Environnement, École Nationale Supérieure des Mines d'Albi-Carmaux, Institut National Polytechnique de Toulouse, France, 2014.
- [23] A. Mersmann, Crystallization Technology Handbook, 2e éd., Marcel Dekker, New York, 2001.